

Detailed structure of the H-N-H center in GaAs_yN_{1-y} revealed by vibrational spectroscopy under uniaxial stress

L. Wen,¹ F. Bekisli,¹ M. Stavola,^{1,*} W. B. Fowler,¹ R. Trotta,² A. Polimeni,² M. Capizzi,² S. Rubini,³ and F. Martelli³

¹Department of Physics and Sherman Fairchild Laboratory, Lehigh University, Bethlehem, Pennsylvania 18015, USA

²CNISM and Dipartimento di Fisica, Sapienza Università di Roma, I-00185 Roma, Italy

³Laboratorio Nazionale TASC, INFN-CNR, Area Science Park, Strada Statale 14, Km. 163.5, I-34012 Trieste, Italy

(Received 17 April 2010; published 2 June 2010)

The H-N-H center in GaAs_{1-y}N_y that is responsible for the band-gap shift caused by H has been studied by infrared spectroscopy in conjunction with uniaxial stress and by theory. Rich, microscopic details about its canted structure are obtained. The splitting of the infrared lines confirms the C_{1h} symmetry of the defect and yields a quantitative value for the canting angle of the center. The reorientation barrier of the defect is estimated from stress-induced reorientation at temperatures near 30 K to be 96 meV.

DOI: [10.1103/PhysRevB.81.233201](https://doi.org/10.1103/PhysRevB.81.233201)

PACS number(s): 61.72.Bb, 63.20.Pw, 78.30.Fs

The addition of a few percent N causes a large reduction in the band gap of the dilute III-N-V alloys GaAs_{1-y}N_y and GaP_{1-y}N_y.^{1,2} The further introduction of H into these dilute alloys causes the band gap of the nitrogen-free host to be recovered.³⁻⁶ These remarkable effects have stimulated considerable research on the basic physics of these materials and their application in optoelectronic devices and for the fabrication of nanostructures.^{1,2,7-9}

Vibrational spectroscopy of the light elements N and H in conjunction with theory has provided an excellent strategy for probing the microscopic structures of the defects responsible for the unusual band-gap shift of the dilute III-N-V alloys caused by H.^{10,11} The infrared (IR) absorption spectrum of GaAs_{1-y}N_y:H shows strong absorption lines at 1447 (1076), 2967 (2217), and 3195 (2376) cm⁻¹. (The deuterium isotope is, in fact, more convenient for our studies and gives the vibrational frequencies that are shown in parentheses.) An IR study of GaAs_{1-y}N_y that had been treated with both H and D revealed that the defect causing the recovery of the band gap gives rise to two inequivalent, weakly coupled N-H stretching modes.¹⁰

Several groups performed calculations that initially suggested nitrogen-stabilized H₂* structures with one H atom at a bond-centered site and a second H at an antibonding site along the same <111> axis to explain the band-gap shifts caused by H.¹²⁻¹⁷ However, these H₂(N) structures were found to be inconsistent with the vibrational properties of GaAs_{1-y}N_y:H that were subsequently measured.^{10,11} Alternative H-N-H structures with C_{2v} symmetry or with a canted C_{1h} geometry (Fig. 1) have been proposed.¹⁹⁻²¹ The observed vibrational properties are most consistent with the canted H-N-H structure with C_{1h} symmetry. The 2967 and 3195 cm⁻¹ lines have been assigned to two weakly coupled N-H modes of the H-N-H defect and the 1447 cm⁻¹ line has been assigned to an in-plane wagging mode.¹¹

While a canted H-N-H defect can explain the observed IR properties, its structure has been challenging to probe experimentally and has remained controversial. A study of GaAs_{1-y}N_y:H by x-ray absorption near-edge structure spectroscopy (XANES) and theory found that defects with C_{2v} or “asymmetric C_{2v}” symmetry are consistent with the observed XANES spectra.^{21,22} And a recent IR study has proposed that

the two N-H stretching modes are associated with different defects²³ (although the critical experiments on defects containing both H and D that revealed the coupling of these N-H modes were not performed in this study). There is also evidence for related defects that contain three or four hydrogens.²⁴⁻²⁶ In the present paper, the perturbation of the vibrational properties of GaAs_{1-y}N_y:D by uniaxial stress provides an elegant experimental strategy for verifying the D-N-D structure proposed by theory and for revealing rich, microscopic detail about its canted structure.

A GaAs_{1-y}N_y epitaxial layer was grown by plasma-assisted, solid-source molecular-beam epitaxy on an undoped (001) GaAs substrate. A 2-μm-thick GaAs_{1-y}N_y layer with y=0.15% was grown on a 1-μm-thick GaAs buffer layer. The substrate was 2 mm thick so that samples suitable for uniaxial stress measurements could be prepared. Hydrogenation or deuteration of samples was performed with a Kaufman ion source with samples held at 300 °C. The ion energy was 100 eV and current densities of ~10 μA/cm² were used. Photoluminescence measurements were performed to confirm the band-gap shifts caused by H or D. Following hydrogenation at 300 °C, epitaxial GaAs_{1-y}N_y has been found to have the lattice constant of the GaAs substrate.²⁶

IR absorption spectra were measured with a Bomem DA.3 Fourier-transform spectrometer equipped with a KBr

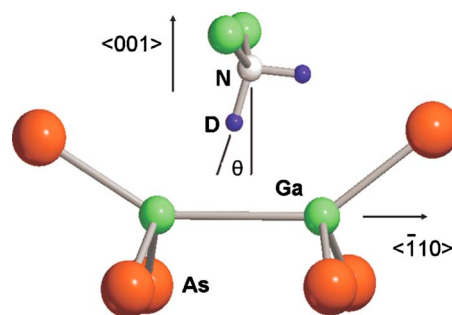


FIG. 1. (Color online) The relaxed D-N-D defect in GaAs_{1-y}N_y (Ref. 18). The angle, θ , of the N-D bond of the defect that gives rise to the 2217 cm⁻¹ line is measured with respect to the <001> axis that is perpendicular to the <110> primary symmetry axis of the C_{1h} center.

beam splitter and an InSb detector. The IR frequency range near 2250 cm^{-1} , where the D-stretching modes occur, yields spectra with a substantially greater signal-to-noise ratio than the frequency range where the corresponding H modes occur; therefore, we have chosen to focus primarily on the D-N-D complex. Uniaxial stress was applied with a push rod apparatus that was cooled in an Oxford CF 1204 cryostat using He contact gas. The probing light was polarized with a wire grid polarizer that was placed in the IR beam path after the cryostat. $\text{GaAs}_{0.9985}\text{N}_{0.0015}$ samples for stress experiments were prepared with dimensions $2 \times 3.5 \times 12\text{ mm}^3$. For samples with an aspect ratio $> 3:1$ and end surfaces carefully prepared to be flat and parallel, the stress in the center section of the sample where IR measurements are made is uniaxial throughout its thickness. For an epitaxial layer grown on a (001) substrate, samples could be prepared for stresses to be applied along [100] or [110] directions and with the probing light incident along the [001] direction.

Theoretical calculations were performed as extensions of those reported in Refs. 11 and 19 and were carried out with the CRYSTAL2006 code²⁷ using density-functional theory with a gradient-corrected approximation to the exchange-correlation functional (Becke exchange²⁸ with 20% Hartree-Fock, Lee-Yang-Parr correlation,²⁹ 90% nonlocal exchange, 81% nonlocal correlation; potential B3LYP). The calculations were carried out in a periodic supercell with two hydrogen impurities and 54 host atoms with a computed GaAs lattice constant of 5.77 \AA . A $4 \times 4 \times 4$ k -point mesh of Monkhorst-Pack³⁰ type was used. The self-consistent-field energy convergence criterion was 10^{-7} hartree.

Gaussian basis functions³¹ were of the type $s(3)s(1)s(1)sp(1)$ for hydrogen and $s(7)sp(3)sp(1)sp(1)$ for nitrogen. For gallium and arsenic, most of the calculations utilized Barthelet-Durand³² pseudopotentials, with corresponding basis functions.

Two different types of stress experiments have been performed.^{33,34} In the first set of experiments, stress is applied to samples at 4.2 K where we have found the D-N-D center to be static and unable to reorient among its possible configurations on the time scale of the IR measurements. The applied stress causes centers along directions that have been made inequivalent to have different vibrational frequencies. In the second set of experiments, stress is applied at elevated temperatures to probe whether the D-N-D center is able to reorient.

Figure 2 shows spectra of the 2217 cm^{-1} line of the D-N-D complex for $\text{GaAs}_{0.9985}\text{N}_{0.0015}:\text{D}$ samples with stresses applied along the [110] and [100] directions.³⁵ The second derivatives of these spectra are also shown to help reveal the stress-induced splittings that have been found. For the [110] stress direction, the 2217 cm^{-1} line is split into two components (e_1 and e_2) that are seen for both polarizations of the probing light. For the [100] stress direction, the 2217 cm^{-1} line is again split into two components (a and b) with the component shifted to lower frequency (a) seen primarily for the polarization parallel to the stress and with the component shifted to higher frequency (b) seen primarily for the polarization perpendicular to the stress. To determine the positions and relative intensities of the stress-split components, we have fit the spectra shown in Fig. 2 with Pearson

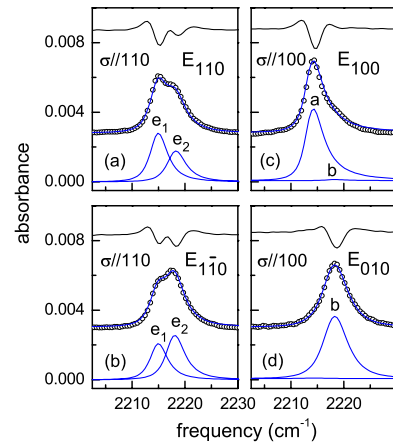


FIG. 2. (Color online) Effect of stress applied along the [110] and [100] directions for the 2217 cm^{-1} line of the D-N-D defect in $\text{GaAs}_{0.9985}\text{N}_{0.0015}$. Spectra (shown by open circles) were measured near 4 K with a resolution of 1 cm^{-1} . The results of fits to the individual split components are shown by the solid line superposed on the measured IR data. The upper trace in each panel shows the second derivative of the measured spectrum. The incident light was polarized with the directions of the electric vector that are shown. The magnitudes of the stresses along the [110] and [100] directions were 230 MPa and 250 MPa, respectively.

IV line shapes³⁶ to account for the observed asymmetry of the lines. A fit was first made to a spectrum measured at zero stress to determine the asymmetry parameters of the line shape. The fits shown in Fig. 2 were then made for spectra measured under stress using the same asymmetry parameters. The other N-H(D) lines in the IR spectrum are affected only weakly by stress and did not show splittings that could be resolved.

The symmetry of the center and the direction of its transition moment can be determined from the number of stress-split components and their relative intensities. The stress-splitting patterns for centers with different point groups are given in the classic work of Kaplyanskii.³⁷ Results for defects with the C_{1h} point group are of particular interest here and are given by Davies *et al.*³⁸ For the spectra shown in Fig. 2, the number of components and their relative intensities are characteristic of the C_{1h} point group. A center with the C_{1h} point group has a primary axis along the $\langle 110 \rangle$ direction that is normal to the reflection plane of the center (for the defect being studied here in the direction normal to the plane of the D-N-D center shown in Fig. 1). A transition moment for an electric dipole transition can be oriented along the main symmetry axis or can lie in the reflection plane that is normal to this axis (i.e., in the plane of the D-N-D center) without any further restriction on angle imposed by symmetry. The relative intensities of the stress-split components have been determined by Davies *et al.*³⁸ as a function of the angle θ of the transition moment in the reflection plane. The angle θ is measured with respect to the $\langle 001 \rangle$ direction that is perpendicular to the $\langle 110 \rangle$ primary axis of the defect.

The shift rates of the components of a C_{1h} center that can be studied with the sample orientations available to us are shown in Table I. The line splittings for a C_{1h} center can be characterized by four shift rates, A_1 , A_2 , A_3 , and A_4 .

TABLE I. Uniaxial stress perturbations for a C_{1h} center for the [100] and [110] stress directions and a [001] viewing axis. The columns on the right give the theoretical results for the intensities of the stress-split absorption lines for specific angles of the transition moment direction that lies in the plane that is normal to the main $\langle 110 \rangle$ symmetry axis of a C_{1h} center. Results are given for $\theta=0^\circ$ (left column) and $\theta=7^\circ$ (right column), where θ is the angle between the transition moment direction and the (001) axis perpendicular to the $\langle 110 \rangle$ symmetry axis of the center. See Ref. 38.

Stress	Component	Shift rate	$E_{\parallel 100}:E_{\parallel 010}$	
[100]	a	A_1	4:0	3.9:0.03
	b	A_2	0:4	0.06:4.0
			$E_{\parallel 110}:E_{\parallel 1\bar{1}0}$	
[110]	e_1	$(A_1+A_2)/2-A_4$	2:2	2.3:1.6
	e_2	$(A_1+A_2)/2+A_4$	2:2	1.6:2.3
	f	A_2-A_3	0:0	0.03:0.03
	g	A_2+A_3	0:0	0.03:0.03

From our data, we find $A_1 = -6.4 \pm 2 \text{ cm}^{-1}/\text{GPa}$, $A_2 = 9.6 \pm 2 \text{ cm}^{-1}/\text{GPa}$, and $A_4 = 6.9 \pm 2 \text{ cm}^{-1}/\text{GPa}$. A_3 cannot be determined from our data because the components g and f have intensities too small to be seen for the sample orientations used in our experiments (see Table I). The sign of A_4 can be positive or negative.

The angle of the transition moment can be determined from the relative intensities of the stress-split components and the results reported by Davies *et al.*³⁸ We find that the relative intensities of the components shown in Fig. 2 are consistent with a transition moment lying in the D-N-D plane and oriented with an angle θ of only a few degrees (see Table I). The two components, e_1 and e_2 , seen for the [110] stress direction have relative intensities of 1.45:1 for $E_{\parallel 110}$ and of 1:1.36 for $E_{\parallel 1\bar{1}0}$. These relative intensities yield a transition moment with angle $\theta = 7^\circ \pm 4^\circ$. (The calculated intensity ratio, 2.3/1.6, shown in Table I for the e_1 and e_2 components of a C_{1h} center³⁸ with $\theta=7^\circ$ is equal to 1.4/1, consistent with our experimental data. The error in the angle θ was determined from an estimate of the error in the intensity ratios determined from the fits to the line shapes seen for [110] stress.) For θ small, the intensities of the components f and g are predicted to be negligibly small, consistent with our results. For the [100] stress direction, we have used the predicted relative intensities of the a and b components for $\theta=7^\circ$ (Table I) to produce a satisfactory fit to the spectra shown in Figs. 2(c) and 2(d).

Previous IR results for the D-N-D center where one of the D atoms was replaced by H showed that the frequencies of the dynamically decoupled modes of the D-N-H and H-N-D centers were shifted by only a few inverse centimeters. This experimental result is characteristic of two inequivalent N-D modes that are only weakly coupled, a conclusion that is consistent with model calculations of the D-N-D center's vibrational properties.^{10,11} In this case, an independent oscillator model is appropriate and the angle of the transition moment reveals the angle θ of the N-D bond of the D-N-D

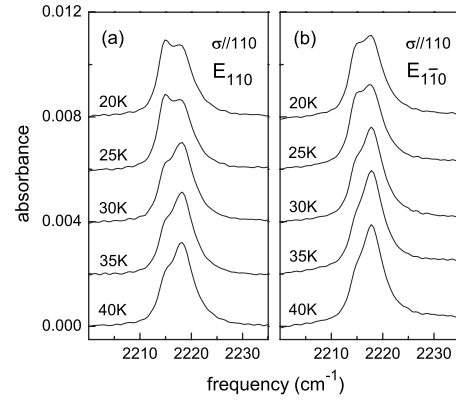


FIG. 3. Effect of [110] stress (230 MPa) on the relative intensities of the components of the 2217 cm^{-1} line of the D-N-D center in $\text{GaAs}_{0.9985}\text{N}_{0.0015}$. Stress was applied initially at 4 K. The sample was then annealed for 30 min with the stress maintained at the successively higher temperatures that are shown. The infrared spectra shown were measured at 4 K with polarized light following each anneal.

center shown in Fig. 1. The angle $\theta = 7^\circ \pm 4^\circ$ found from experiment may be compared with a value of $18^\circ \pm 6^\circ$ predicted from CRYSTAL06 calculations.

When [110] stress is applied at elevated temperature, we have discovered that the relative intensities of the e_1 and e_2 components are changed due to a stress-induced alignment of the differently oriented components of the C_{1h} D-N-D center (Fig. 3). The alignment produced by [110] stress occurs because the e_2 and e_1 orientations have different ground-state energies under stress, a result that is also consistent with the C_{1h} symmetry of the defect. These e_1 and e_2 components are then populated according to their Boltzmann factors if sufficient time is allowed for equilibrium to be established. Similar experiments performed for [100] stress did not produce a change in the relative intensities of the a and b components shown in Figs. 2(c) and 2(d), even for stresses applied at temperatures as high as room temperature.

The discovery of a defect alignment produced by [110] stress creates an opportunity to probe experimentally the energy lowering that results from the canting distortion of the D-N-D center. To study the kinetics of the formation of this alignment, a sample was cooled to 4 K prior to the application of [110] stress at low temperature. This sample was then annealed at successively higher temperatures with the stress maintained. After each 30 min anneal, the sample was cooled to 4 K for the measurement of an IR spectrum. The results of these experiments are shown in Fig. 3 where it is seen that a 30 min anneal at 30 K produces a pronounced alignment of the D-N-D center. The alignment is complete after the anneal at 35 K and no further alignment was produced for anneals performed with the stress maintained at higher temperatures. An analysis of the data shown in Fig. 3 yields an alignment of $[I(e_2) - I(e_1)]/[I(e_2) + I(e_1)] = 0.4$ for a [110] stress of 230 MPa applied for 30 min at 40 K. $I(e_1)$ and $I(e_2)$ are the intensities of the absorption lines for the e_1 and e_2 components, summed over the parallel and perpendicular polarizations, determined from fits to the line shapes.

For the C_{1h} model of the D-N-D center shown in Fig. 1,

there are 12 possible center orientations.^{37,38} For the [110] stress direction, four of these orientations give rise to the f and g components that are not seen in our experiments. The remaining eight orientations are broken into two groups, e_1 and e_2 . For the e_1 and e_2 components, the $\langle 110 \rangle$ primary axes of these defect orientations make the same angle (60°) with respect to the [110] stress axis. For the model shown in Fig. 1, the e_1 and e_2 components differ in the sign of the cant angle θ . The barrier between these inequivalent orientations is determined by the energy of the relaxed symmetric configuration, for which θ is predicted to be half of 96.9° , or 48.45° .

The rate, k , for the production of an alignment by [110] stress is determined by the energy barrier between the inequivalent orientations and has been found to be $0.77 \times 10^{-3} \text{ s}^{-1}$ (30 K) from the data shown in Fig. 3. This rate is assumed to be due to thermally activated hopping over the barrier between orientations and is given by the relationship,

$$k = \nu_0 \exp(-E_A/k_B T). \quad (1)$$

The attempt frequency is taken to be $\nu_0 = 10^{13} \text{ s}^{-1}$, a value that is typical of a phonon frequency in GaAs.³⁹ The barrier

height E_A is estimated to be 96 meV from Eq. (1) and the reorientation rate found at 30 K. This may be compared with a predicted value from CRYSTAL06 of 120 meV as the difference between the relaxed C_{2v} defect configuration and the zero-point energy of the relaxed canted state.⁴⁰

In conclusion, IR spectroscopy in conjunction with uniaxial stress provides an experimental probe of the D-N-D center in $\text{GaAs}_{1-y}\text{N}_y$ that reveals quantitative microscopic detail about its structure. The D-N-D center is canted to produce a structure with C_{1h} symmetry. The discovery of stress-induced alignment and the study of its formation kinetics show that the canting distortion of the D-N-D center produces an energy lowering of 96 meV. These results provide an experimental confirmation of the predictions of density-functional theory for the microscopic properties of the D-N-D center in $\text{GaAs}_{1-y}\text{N}_y$:D that is responsible for the remarkable shift of the band gap.

We are grateful to G. D. Watkins and G. Davies for helpful discussions. Work performed at L.U. was supported by NSF under Grant No. DMR 0802278.

*Author to whom correspondence should be addressed; michael.stavola@lehigh.edu

¹ *Dilute Nitride Semiconductors*, edited by M. Henini (Elsevier, Amsterdam, 2005).

² *Physics and Applications of Dilute Nitrides*, edited by I. A. Buyanova and W. M. Chen (Taylor & Francis, New York, 2004).

³ A. Polimeni *et al.*, *Phys. Rev. B* **63**, 201304(R) (2001).

⁴ A. Polimeni *et al.*, *Physics and Applications of Dilute Nitrides* (Ref. 2), Chap. 6.

⁵ A. Polimeni *et al.*, *Phys. Rev. B* **67**, 201303(R) (2003).

⁶ I. A. Buyanova *et al.*, *Phys. Rev. B* **70**, 245215 (2004).

⁷ M. Felici *et al.*, *Adv. Mater.* **18**, 1993 (2006).

⁸ R. Trotta *et al.*, *Appl. Phys. Lett.* **92**, 221901 (2008).

⁹ L. Felisari *et al.*, *Appl. Phys. Lett.* **93**, 102116 (2008).

¹⁰ F. Jiang *et al.*, *Phys. Rev. B* **69**, 041309(R) (2004).

¹¹ S. Kleekajai *et al.*, *Phys. Rev. B* **77**, 085213 (2008).

¹² P. Dixon *et al.*, *Phys. Status Solidi B* **210**, 321 (1998).

¹³ A. Janotti *et al.*, *Phys. Rev. Lett.* **88**, 125506 (2002).

¹⁴ Y.-S. Kim *et al.*, *Phys. Rev. B* **66**, 073313 (2002).

¹⁵ A. Janotti *et al.*, *Phys. Rev. Lett.* **89**, 086403 (2002).

¹⁶ A. Amore Bonapasta *et al.*, *Phys. Rev. Lett.* **89**, 216401 (2002).

¹⁷ A. Amore Bonapasta *et al.*, *Phys. Rev. B* **68**, 115202 (2003).

¹⁸ P. Ugliengo *et al.*, *Z. Kristallogr.* **207**, 9 (1993); P. Ugliengo, "MOLDRAW: A program to display and manipulate molecular and crystal structures," Torino, 2006, available on the web at <http://www.moldraw.unito.it>

¹⁹ W. B. Fowler *et al.*, *Phys. Rev. B* **72**, 035208 (2005).

²⁰ M.-H. Du *et al.*, *Phys. Rev. B* **72**, 073202 (2005).

²¹ G. Ciatto *et al.*, *Phys. Rev. B* **71**, 201301(R) (2005).

²² G. Ciatto *et al.*, *Phys. Rev. B* **79**, 165205 (2009).

²³ H. C. Alt *et al.*, *Phys. Status Solidi B* **246**, 200 (2009).

²⁴ I. A. Buyanova *et al.*, *Appl. Phys. Lett.* **90**, 021920 (2007).

²⁵ A. Amore Bonapasta *et al.*, *Phys. Rev. Lett.* **98**, 206403 (2007).

²⁶ M. Berti *et al.*, *Phys. Rev. B* **76**, 205323 (2007).

²⁷ R. Dovesi *et al.*, *Crystal06 User's Manual* (University of Torino, Torino, 2006).

²⁸ A. D. Becke, *Phys. Rev. A* **38**, 3098 (1988).

²⁹ C. Lee *et al.*, *Phys. Rev. B* **37**, 785 (1988).

³⁰ H. J. Monkhorst *et al.*, *Phys. Rev. B* **13**, 5188 (1976).

³¹ Basis functions were obtained from the web site of M. D. Towler, <http://www.tcm.phy.cam.ac.uk/~mdt26/crystal.html>

³² P. Durand *et al.*, *Theor. Chim. Acta* **38**, 283 (1975); J. C. Barthelat *et al.*, *Gazz. Chim. Ital.* **108**, 225 (1978).

³³ M. Stavola, in *Identification of Defects in Semiconductors*, edited by M. Stavola (Academic Press, San Diego, 1999), Chap. 3, p. 153.

³⁴ Similar stress experiments were performed for the Be-H complex in GaAs. M. Stavola *et al.*, *Phys. Rev. B* **39**, 8051 (1989).

³⁵ The width of the 2217 cm^{-1} line that was observed for $\text{GaAs}_{1-y}\text{N}_y$ samples studied previously with $y=0.007$ was $\approx 9 \text{ cm}^{-1}$ and did not permit stress-induced line splittings to be well resolved (Ref. 11). The linewidths of the 2217 cm^{-1} line for the samples studied here with $y=0.0015$ are $\approx 4.3 \text{ cm}^{-1}$ and have allowed the splittings of this IR line under stress to be studied.

³⁶ PEAKFIT, Peak Separation and Analysis Software for Windows, Jandel Scientific Software, San Rafael, California, 1995.

³⁷ A. A. Kaplyanskii, *Opt. Spectrosc.* **16**, 329 (1964).

³⁸ G. Davies *et al.*, *Phys. Rev. B* **35**, 2755 (1987).

³⁹ The barrier height is insensitive to the value of the attempt frequency and changes by only $\approx 10 \text{ meV}$ if the attempt frequency is changed by a factor of 100.

⁴⁰ Du *et al.* (Ref. 20) obtained a theoretical barrier height of 50 meV using a local-density approximation Hamiltonian.